

Impact of the Pacific-Japan pattern on the tropical Indo-western Pacific Ocean Surface Waves

Srinivas G^{1*}, Remya P. G²., Subhra Prakash Dey¹, Jasti S. Chowdary³ and Prashant Kumar⁴

¹CSIR – National Institute of Oceanography, Dona Paula, Goa, India

²ESSO-Indian National Centre for Ocean Information Services, Hyderabad, India

³ESSO-Indian Institute of Tropical Meteorology, Pune, India

⁴Department of Applied Sciences, National Institute of Technology, Delhi, India

Corresponding Author:Dr. Srinivas Gangiredda,

Email: srinivasg@nio.org

Abstract

The present study examines the impact of the Pacific-Japan (PJ) pattern on tropical Indo–Western Pacific Ocean significant wave heights during the boreal summer season (June through August, JJA) for the first time. The PJ pattern is a dominant teleconnection pattern characterized by meridional propagating Rossby waves over the Western North Pacific (WNP) and East Asia. The strong southwesterly monsoon winds prevail over the North Indian Ocean (NIO) during JJA inducing strong wave heights in the mean state. The regression analysis of significant wave height anomalies on the PJ index exhibits strong negative wave height anomalies over the Bay of Bengal (BoB), the tropical WNP region and slightly weaker negative anomalies over the Arabian Sea (AS) due to a reduction in the wind-wave growth. The weakening of wave heights in the BoB and WNP regions during PJ is attributed to the anomalous low-level anticyclonic circulation accompanied by high sea-level pressure anomalies over the BoB and WNP regions. The anomalous anticyclonic circulation opposes the mean south-westerlies and reduces the wave heights over the NIO and WNP. Further, the composite analysis of positive and negative PJ patterns display significant asymmetries in their signature on the wind and wave parameters. Thus, our findings suggest that the WNP region's climate conditions strongly modulate the NIO's surface waves.

Keywords Significant Wave Heights, Pacific-Japan pattern, anomalous anticyclonic circulation, North Indian Ocean, Western North Pacific.

1. Introduction

The Indo–Western Pacific Ocean region is known for hosting several coupled air-sea processes consisting of the Asian monsoon system maritime continent convection, and the warm pool region (e.g., Webster et al. 1998, Chen et al. 2023). The Asian summer monsoon onset starts in May, with the strong cross-equatorial flow off the Somali Peninsula. After that, the monsoonal winds eventually prevail in the North Indian Ocean (NIO) and the Western North Pacific (WNP) (e.g., Schott and McCreary, 2001, Hu et al. 2022). During the boreal summer months (June through August; JJA), the Indian monsoon is the dominant air-sea coupled system. In JJA, the Indo-western Pacific Ocean experiences peak ocean surface gravity wave activity (e.g., Srinivas et al. 2020; Kaur et al. 2021). The surface wind climate in the NIO is directly influenced by the summer monsoon circulation, and the monsoon wind pattern over the Arabian Sea (AS) is particularly complex (e.g., Anoop et al. 2015). Coastal and offshore infrastructures, navigation, and coastal dynamics are all impacted by monsoon waves. Therefore, it is important to acknowledge the considerable impact of monsoon waves on the coastal areas of these regions for various applications. Researchers indicate that wave heights in the NIO can reach as high as ~6 m and that monsoon waves are a key driver of coastal erosion and flooding events along the west coast of India (e.g., Kumar et al., 2006).

The tropical Indian Ocean (TIO) surface waves exhibit variability across different timescales ranging from intraseasonal to interannual periods (e.g., Hemer et al. 2013; Srinivas et al. 2020; Remya et al. 2020). In the interannual timescales, wave variability in the TIO is driven by potential factors such as the Indian Ocean Dipole (IOD), El Niño Southern Oscillation (ENSO), and Southern Oscillation Mode (SAM). Recent studies have shown that IOD impacts the AS surface waves (Anoop et al. 2016), while ENSO's influence on global ocean waves (e.g., Hemer et al. 2010; Kumar et al. 2016). The IOD events alter the wind patterns which influence the generation and dissipation of surface waves over the AS by changing the pressure gradient over the region (Anoop et al., 2016). The significant wave height in the TIO is modulated by the swells coming from the Southern Ocean generated by the westerlies over 40 – 60°S which have a strong connection with ENSO and SAM (Remya et al., 2020). The swells generated by south-easterlies over the eastern TIO, controlled by the ENSO, also contribute to the significant wave height in the NIO. Several studies have demonstrated the influence of SAM on global ocean surface wave heights (e.g., Marshall. 2003; Hemer et al. 2010; Marshall et al. 2018). All these climate modes modulate the winds and thereby the wave climate in the TIO (e.g., Srinivas et al. 2021; Remya et al. 2020). Identifying the dominant climate modes that impact the tropical Indo-Western Pacific Ocean surface wave variability is crucial. One of the important climate modes over the Indo-Western Pacific region is the Pacific-Japan (PJ) pattern, which is a low-

level circulation variability mode in the WNP region (Nitta, 1987; Kosaka 2021, Noh et al. 2021, Hu et al. 2024). This mode is known to have a significant impact on atmospheric circulation and rainfall over the Indo-western Pacific region (Xie et al. 2016; Srinivas et al. 2018, Hu et al. 2024).

The Indian Ocean-Western Pacific variability plays an important role, especially in the regional climate. Many recent studies have highlighted the interaction between the PJ pattern and Indian Ocean Sea Surface Temperatures (SST) (e.g., Kosaka et al. 2013; Srinivas et al. 2018; Chowdary et al., 2019, Kosaka 2021) and this association is referred to as the Indo-Pacific Ocean Capacitor (IPOC) mode (Xie et al. 2016, Du et al. 2022). The boreal summer SST warming in the NIO, the anomalous anticyclonic circulation over the WNP, and SST cooling in the WNP during boreal spring and early summer are essential parts of IPOC (Xie et al., 2016) and PJ pattern (Kosaka et al. 2013). Previous studies highlighted the PJ pattern as the dominant mode of climate variability in the WNP during JJA is known to have a significant impact on atmospheric circulation and rainfall, as well as on the ocean circulation (e.g., Nitta 1987; Huang and Sun 1992; Kosaka et al. 2013; Kubota et al. 2016; Srinivas et al. 2018, Hu et al. 2024). The PJ pattern features a meridional dipole structure in lower-tropospheric circulation and precipitation anomalies with the tropical and midlatitude WNP lobes (Nitta 1987; Kosaka and Nakamura 2010) and provides a crucial link between the tropics and midlatitudes. The positive PJ pattern is significantly correlated with the decay phase of El Niño (e.g., Sun et al. 2010; Xie et al. 2016, Kosaka 2021). On the other hand, the negative phase of the PJ pattern causes droughts and heat waves in the midlatitudes with enhanced tropical cyclone activity over the WNP region (e.g., Kosaka et al. 2013).

For the recent three decades, the PJ has been known to well correlate with ENSO in the preceding boreal winter and Indian Ocean SSTs in the concurrent summer (e.g., Kubota et al. 2016, Hu et al. 2024). The positive phase of PJ enhances the summer monsoon rainfall over the southern and northern parts of India through northeastward atmospheric Rossby wave propagation from the tropical WNP, while the negative phase suppresses the precipitation (e.g., Srinivas et al., 2018; Hu et al. 2024). It is found that the positive rainfall band over north India is due to anomalous low-level moisture convergence in the north-western edge of the westward propagating atmospheric cold Rossby wave as a response to suppressed convection over the tropical WNP region associated with the PJ pattern. This highlights the importance of the atmospheric pathway that connects the PJ and NIO circulation. Though the PJ pattern has a profound impact on the Indian summer monsoon, there is no study depicting the influence of the PJ pattern on the NIO surface waves. Thus, the present study addresses the PJ influence on the Indo-Western Pacific Ocean wave heights. The rest of the paper is organised as follows: Section 2 outlines the data used for analysis, as well as the methodologies. In Section 3,

we examine the PJ mode influence on the Indo–Western Pacific Ocean surface waves and changes in the mean-state climatology. Section 4 features the positive and negative PJ patterns asymmetrical response of wind and waves. Finally, in Section 5, we summarise the key takeaways from our analysis.

2. Data and methods

We utilize the European Centre for Medium-Range Weather Forecasts (ECMWF) reanalysis (ERA5), the fifth-generation ECMWF reanalysis that replaces the ERA-interim reanalysis (Hersbach et al., 2020). ERA5 merges model data with observations from around the world using the laws of physics and data assimilation techniques to provide a complete and consistent global dataset. It offers hourly estimates for a large number of quantities related to the atmosphere, ocean waves, and land surface with a horizontal resolution of $0.25^{\circ} \times 0.25^{\circ}$ for the atmosphere and $0.5^{\circ} \times 0.5^{\circ}$ for ocean waves. Here, we use the monthly averages of significant wave height (Hs), wind-seas (Hsw), swell wave heights (Hss), mean wave period (Tp), wind wave period (Tpw) and swell wave period (Tps) from ERA5 data from 1959-2021 with a horizontal resolution of $0.5^{\circ} \times 0.5^{\circ}$. In addition, we also obtained the atmospheric parameters such as surface zonal and meridional wind components, and mean sea level pressure (SLP). To understand how wind energy is transferred into waves, we use the normalized energy flux transfer into waves from ERA5. A positive flux indicates a flux into the waves, and it has units of W/m^2 , normalized by dividing it by the product of air density and the cube of the friction velocity.

An empirical orthogonal function (EOF) analysis was applied on 850 hPa relative vorticity anomalies over 0° – $60^{\circ}N$, 100° – $160^{\circ}E$ during the boreal summer season (JJA) to extract the PJ pattern as the dominant mode of lower-tropospheric circulation variability over the WNP and East Asia regions. This methodology corroborates with studies by Srinivas et al. (2018), and Kosaka et al. (2013), albeit with a focus on the interannual variability of seasonal-mean anomalies. Statistical methods such as correlations, regressions and composite analysis are used.

3. The PJ influence on the tropical Indo-western Pacific Ocean surface waves

Many past studies show that the PJ influences the Indian summer monsoon rainfall, TIO SST and low-level circulation (e.g., Kosaka 2021; Srinivas et al. 2018). For the first time, we explore the PJ impact on Indo-western Pacific Ocean surface gravity waves during JJA. Before, proceeding with the understanding of the relationship between PJ and ocean waves, we benchmark the climatological mean-state features of surface winds and ocean wave parameters in the tropical Indo-western Pacific region during JJA. Figure 1 shows the seasonal means of surface wind, Hs, Hsw and Hss, and their wave periods during JJA. The predominant southwesterly monsoon winds with a speed of more than 10-12 m/s in the AS and 8-10 m/s over the Bay of Bengal (BoB) cover the entire NIO, resulting in

mean wave heights of more than 3m and 2m over the respective regions (Fig. 1a, b). In AS, the strong winds are due to the southwest monsoon winds driven by the pressure gradients between the Indian Ocean and the Indian land mass. H_s is mostly dominated by the wind-sea, with a minimal contribution from the swells over AS, whereas in BoB the contribution of seas and swells are almost equal in JJA. T_p ranges from 8 to 10s in AS, which is shorter when compared to the rest of the basin (10-11s), indicating the dominance of the wind-sea (Fig. 1c). Previous studies have demonstrated a strong correlation between surface wind and wave conditions over the AS during boreal summer months, as these regions are sheltered from distant swells and are dominated by wind waves locally (e.g., Anoop et al. 2016). The tropical Southern Indian Ocean displays mean wave heights ranging from 3-4m with a wave period of more than ~ 10 s, suggesting the propagation of swells from the southern Indian Ocean (Fig. 1b-d). Recent studies have shown that Southern Ocean swells are one of the important factors affecting the wave climate of NIO (e.g., Remya et al., 2016; Sreejith et al. 2023). They also reported that SAM is the strongest mode of variability which alters the strength and distribution of southern swells and also influences the behaviour and distribution of NIO swells. Another potential source of generating swells is easterly Jets located at 20°S which peaks during boreal summer. The BoB is most affected by swells compared to AS due to the direction and orientation of swell propagation from the south. The WNP exhibits lower wave heights due to weak climatological northeasterly winds (Fig. 1a). During the In boreal summer months, the TIO surface waves exhibit profound interannual variability and stronger magnitudes, primarily induced by wind changes (e.g., Srinivas et al. 2020).

Figure 2 presents the PJ pattern extracted by applying the EOF analysis on 850-hPa relative vorticity anomalies in the WNP region during JJA. The method employed in this study has been extensively described and used in prior research (e.g., Nitta 1987; Kosaka et al. 2013; Kuboto et al. 2016; Srinivas et al. 2018). The leading EOF pattern identified a tripole pattern with positive vorticity anomalies extending from the equator to 10°N and in the mid-latitudes ($25^\circ\text{--}45^\circ\text{N}$), with negative vorticity anomalies observed at $10^\circ\text{--}25^\circ\text{N}$ in the WNP (Fig. 2a). The correlation of the corresponding leading principal component of relative vorticity with H_s and surface winds reveals an anomalous anticyclonic circulation over the tropical WNP region and north-easterlies in the northern AS and south-westerlies in the southern AS are noted, as part of the PJ pattern (Fig. 2b). The H_s anomalies display a strong negative correlation over WNP and NIO, and a positive correlation in the southwestern Indian Ocean regions. Previous studies have shown a significant correlation between the PJ pattern and El Niño decaying and developing La Niña phases (Srinivas et al. 2018; Xie et al. 2016; Kosaka et al. 2013; Kosaka and Nakamura, 2010). The simultaneous correlation between PJ and Niño3.4 is -0.31, which is significant at the 95% confidence level. The negative H_s anomalies in the

WNP and BoB regions are attributed to the anomalous anticyclonic circulation over these regions. The anomalous north-easterlies in both regions lead to a reduction in wind speed, which, when combined with the mean south-westerlies, hinders wave growth over NIO. The PJ pattern significantly impacts interannual variability in the WNP, South Asian, and East Asian summer monsoons. This pattern is linked to anomalous convection over the maritime continent, which generates a Rossby wave response and an anomalous low-level cyclonic circulation extending northwestward from the forcing (Matsuno 1966; Gill 1980). The enhanced convection over the maritime continent induces enhanced convection over the NIO via the warm Rossby wave (e.g., Srinivas et al. 2018; Hu et al. 2024). Furthermore, the anomalous surface easterlies along the southern flank of the cold Rossby wave weaken the prevailing monsoon westerlies over the summer NIO and warm the SST by reducing the latent heat flux (e.g., Du et al. 2009, 2022; Xie et al. 2009; Chowdary et al. 2017; Darshana et al. 2022). Consequently, the easterly wind anomalies in the WNP and NIO regions are strongly associated with the tropical WNP anomalous anticyclone as a part of the PJ pattern (Fig. 2a, b). Recent studies suggest that the NIO surface waves experience significant changes in different time scales, they are influenced by Indo-Pacific climate modes (Remya et al. 2020; Srinivas et al. 2021; Kumar et al. 2019). The identification of new sources of variability is pivotal for wave forecasting around Indian Ocean rim countries, in addition to the well-known interannual climate modes.

Figures 3 and 4 illustrate the regression patterns of wave parameters H_s , H_{sw} , and H_{ss} , and their corresponding wave periods, in relation to the PJ index respectively. The analysis reveals that H_s display significant negative anomalies in the WNP and BoB regions, while insignificant anomalies are observed in the AS (Fig. 3a). Interestingly, the T_p exhibits contrasting characteristics in WNP and BoB, with negative anomalies in WNP and positive anomalies in BoB, accompanied by insignificant positive anomalies in AS (Fig. 4a). To explain the contrasts in wave periods, features in the BoB and WNP, it is beneficial to analyze the H_{sw} and H_{ss} regression patterns (Fig. 3b, c). H_{sw} reveals significant negative anomalies in the WNP region, as well as in the NIO (Fig. 3b) suggesting the reduction in the wind wave growth in the WNP. The positive PJ events lead to the development of the northeasterly anomalies in the WNP and BoB regions as a part of anomalous anticyclonic circulation (Fig. 5a). The positive SLP anomalies support the strengthening of the north-easterlies in the southern flank of the anomalous anticyclonic circulation in the WNP and BoB (Fig. 5b). These anomalies during a positive PJ result in the reduction of mean wind speed and subsequently decrease the wind-wave growth in the BoB and WNP regions. H_{sw} is supported by the significant negative anomalies in the T_{pw} in both WNP and NIO regions, similar to H_{sw} (Fig. 3b, 4b). The anomalies of normalized vertical energy flux also display significant negative anomalies over the maritime continent and BoB regions

supporting the reduction of Hsw response to PJ (Fig. 5c). Furthermore, the energy flux anomalies are significantly positive over equatorial central Pacific, suggesting that the energy transfer into waves through easterly wind forcing over there. These positive energy flux anomalies in the central Pacific support that the PJ pattern is strongly associated with the decaying phase of El Niño or developing La Nina (Xie et al. 2016, Kosaka 2021).

The regression patterns of Hss and Tps show negative anomalies in the WNP region (Fig. 3c and 4c). The difference in the regression pattern of swell anomalies suggests that the WNP and NIO regions exhibit varying wave characteristics. This can be confirmed through an analysis of the climatological fields in the Indo-Western Pacific region (Fig. 1). For instance, an examination of the climatology of Tp during JJA reveals that the WNP region experiences waves within the range of 4-8 s. This range is indicative of the dominance of wind-sea and the presence of young swells in the region. In contrast, the NIO experiences waves with a period of 8-12 s, which is indicative of a mixed sea state with both wind-sea and long-period swells. The dominance of the Southern Ocean swells approach to NIO, especially in the BoB is a well-established fact that has been addressed in numerous past studies (Sabique et al, 2012, Remya et al, 2012, Zheng et. al, 2018). Consequently, the reduction in wind speed and associated reduction in wind-sea growth leads to the dominance of long-period swells in the NIO, causing positive anomalies in the wave period. On the other hand, in the WNP region, primarily dominated by local winds and waves, positive PJ-induced weaker winds resulted in a reduction in wave growth (Fig. 3a, 5a). The reduction is reflected in both Hs and Tp anomalies.

In short, a positive PJ pattern results in a net reduction of wind-driven wave growth in the Indo-Western Pacific region. This reduction in the wind-sea leads to increased dominance of the swell in the BoB region. The regression analysis is utilized to elucidate the impact of positive PJ. The study by Srinivas et al. (2018) showed the impact of the PJ pattern on Indian summer monsoon rainfall through air-sea interactions in a coupled model. They carried out a sensitivity experiment to excite the idealized PJ pattern by imposing the negative SST anomalies in the tropical WNP using a coupled model. In the control simulation, there is no signature of the PJ pattern which means no presence of anomalous anticyclonic circulation over tropical WNP (Figure not shown). The difference between the control and experiment runs shows the presence of anomalous anticyclonic circulation with reduced surface wind speed anomalies in the WNP and BoB regions (See Fig. 7 in Srinivas et al. 2018). This advocates that the PJ pattern directly influences the significant wave height anomalies over WNP and BoB regions (Figure not shown). Although direct sensitivity tests for the ocean wave model simulations are not included, the coherence of our findings with previous studies provides confidence in the robustness of the presented analysis. However, the response of wave heights to positive and negative PJ remains

unclear from the regression analysis alone, necessitating an exploration of the asymmetrical or symmetrical patterns associated with these phenomena. Thus, in the following section, we have conducted a composite analysis to investigate the asymmetry/symmetry patterns during negative and positive PJ.

4. The PJ asymmetries impact on wind and waves

The positive PJ pattern is closely related to atmospheric and oceanographic variations such as active phases of the Madden–Julian Oscillation (Madden and Julian 1971), warm SST anomalies over tropical WNP and the La Niña conditions in the equatorial eastern Pacific region (e.g., Zhu et al. 2020). In contrast, the negative PJ pattern is associated with preceding TIO basin-wide SST warming caused by the post-El Niño events (Xie et al. 2009; Kosaka 2021) and local negative SST anomalies (Wu et al. 2010). Li et al. (2020) suggested that the periodicity of intraseasonal oscillation could regulate the periodicity of the PJ pattern, indicating a collaborated effect of the ENSO and the intraseasonal oscillation on the formation of a PJ pattern. Thus, the formation of a PJ pattern is closely tied to the tropical atmospheric and oceanographic variabilities. Recent studies have shown that the positive and negative phases of ENSO and IOD display significant asymmetries in their amplitude, phase and durations (e.g., An et al. 2004, 2023, Srinivas et al. 2022). Likewise, the positive and negative phases of PJ also display asymmetries in their formations, amplitudes and low-level circulation variability over WNP (Takemura and Mukougawa, 2022). However, the response of the ocean surface waves to PJ phases has not been studied earlier. Thus, we explore the wave heights and wave periods during the positive and negative phases of the PJ pattern, and their asymmetries in the Indo-Western Pacific Ocean regions during JJA.

Figures 6 and 7 show the composites of mean wave height and wave period anomalies, including seas and swell patterns during the positive and negative phases of PJ. The composite analysis of the positive PJ phase of Hs and Tp reveals a pattern similar to the regression analysis of PJ (Fig. 6a and 7a). WNP shows negative anomalies in both Hs and Tp, linked to the anticyclonic circulation anomalies opposing the mean flow during JJA (Fig. 8a, 1a). In a post-El Niño summer, the NIO is kept warm by the anomalous easterlies on the south flank of the anomalous anticyclonic circulation over WNP, which opposes the prevailing southwest monsoon and reduces the climatological southwesterlies (Du et al. 2009). BoB shows a negative anomaly in Hs and a positive anomaly in Tp indicating the wind-sea reduction caused swell domination. Hs negative anomaly extends to some parts of AS similar to the regression patterns (Fig. 6a, 3a). Hsw also displays negative anomalies which corroborates with Hs, mostly in the southern Bay (Fig. 6b). The normalized energy flux into waves also displays negative anomalies in conjunction with Hsw over there (Fig. 8c). Furthermore, Tpw

anomalies support the positive Hsw anomalies over BoB indicates the wind sea growth (Fig. 7b). On the other hand, the swells display weaker positive anomalies which indicate the advancement of Southern Ocean swells (Fig. 6c, 7c).

The composite analysis of PJ negative years shows prominent anomaly patterns of Hs and Tp compared to PJ positive years (Fig. 6d, 7d). This means that the cyclonic circulation pattern in the WNP is stronger and enhances the wave growth in both WNP and NIO regions, and is supported by positive anomalies of Tp in WNP and negative anomalies of Tp (due to mixed sea state; wind-sea growth leads to a reduction in the Tp) in NIO (Fig 8b, 7d-f). The composites of Hsw show strong positive anomalies and a weaker positive contribution of Hss coinciding with the Hs anomalies suggesting the response to local mixed sea-state in BoB (Fig. 6d-f). Similarly, Tpw shows strong positive anomalies and Tps also show weaker positive anomalies which oppose the Tp anomalies suggesting wind sea domination and weaker positive swell contribution over BoB (Fig 7d-f). Thus, our analysis highlights that wave heights and periods display asymmetries over NIO and WNP regions during the positive and negative PJ years.

The half sum of the composite positive and negative PJ years is used to measure the PJ asymmetries, similar to the study by Srinivas et al. (2022), for the asymmetrical behaviour of ocean waves and other parameters. Figure 9 shows the PJ asymmetries of surface wind, mean significant wave heights, wave periods and normalized energy flux transfer into waves during JJA. Hs shows significant positive anomalies over NIO and WNP regions suggesting the dominant signature of the negative PJ pattern (Fig. 9a). Tp displays strong positive anomalies over the southern tip of India and the eastern equatorial Indian Ocean region in response to the anticyclonic circulation anomalies with high sea-level pressure adjacent to there (Fig. 9c). Interestingly, the asymmetry pattern in the Tp shows positive values in the BoB, suggesting the positive phase's stronger influence on Tp. Notably, the increase in Tp during the positive phase due to the abundance of swells of long wavelength was much higher than its decrease during the negative phase when wind seas were prevalent (Fig. 9b). The PJ asymmetries imply that the negative PJ phase anomalous cyclonic circulation is strong compared to the anomalous anticyclonic circulation during the positive phase and strengthens the mean wind state during JJA over AS (Fig. 9c). The cyclonic circulation and negative SLP asymmetry in the WNP suggest that the negative phase's imprint is stronger than its positive counterpart over tropical WNP. The asymmetrical behaviour of normalized energy flux anomalies to the PJ pattern shows a peculiar dipole pattern on the eastern TIO with negative anomalies on the equator and positive anomalies in the south of the equator (Fig. 9d, 8c). Furthermore, it shows a weaker positive energy flux anomaly over NIO in response to the negative PJ phase. Overall, our analysis suggests that the negative PJ phase is

enhancing the wave growth in the Indo-Western Pacific region, the negative PJ impact on the wave is more important than its counterpart.

5. Summary and Conclusions

This study investigates the impact of the PJ pattern on ocean surface waves in the Indo-western Pacific region during the boreal summer season. Previous research has highlighted the influence of the PJ pattern on various atmospheric and oceanic phenomena, including Indian summer monsoon rainfall, TIO SSTs, and low-level circulation. For this first time, here we explore its impact on ocean surface gravity waves using ERA5 reanalysis data. The study examined the climatological mean-state features of surface winds and ocean wave parameters in the tropical Indo-western Pacific region during JJA. The analysis reveals strong southwesterly monsoon winds over NIO, leading to significant mean wave heights over this region (e.g., Anoop et al. 2016). Wind-sea dominates wave heights in the AS, while both wind-sea and swells contribute equally in the BoB (e.g., Remya et al. 2012). The EOF analysis of 850-hPa relative vorticity anomalies is used to extract the dominant low-level circulation mode over the WNP, which is the PJ pattern during JJA (Nitta, 1987; Kosaka et al. 2013; Srinivas et al. 2018). The PJ pattern exhibits significant correlations with ocean surface wave parameters, particularly showing negative wave height anomalies in the WNP and BoB regions. The regression of the PJ pattern on the significant wave height anomalies over the Indo-western Pacific region shows negative wave height anomalies in the WNP and BoB regions (Fig. 10). This weakening of wave heights is caused by the anomalous anti-cyclonic circulation over the tropical WNP and BoB regions (Fig. 10, red elliptical circle). The northeasterly wind anomalies (curved black arrow) in the southern flank of the anomalous anticyclonic circulation suppress the mean southwesterly winds (grey/white vectors) over the NIO and WNP regions. Thus, it results in the reduction of wind-sea growth and decreases total wave height anomalies over there. The regression analysis shows that the PJ mode negatively influences wind seas over the BoB and has minimal influence on swells over the NIO. Further, it also showed a considerable negative influence on total significant wave height anomalies over the BoB. By performing composite analysis, we found that the anticyclonic wind pattern in the WNP region during the positive phase of the PJ induces anomalous north-easterlies in the BoB and weakens the southwest monsoon winds. The weakening of southwest monsoon winds results in a reduction in wind seas and dominance of swells in the BoB. The abundance of swells in the BoB increases the total wave period up to 0.4 s. It is found that the negative PJ pattern induces anomalous southwesterlies over the BoB which strengthens the mean monsoon winds. The stronger winds in the BoB produce wind-seas which results in an elevation of total SWH up to 0.16 m. Generally, the significant wave heights reach up to 6m on the Indian coast during the Indian summer monsoon season and in addition to this, elevation

induced by the negative PJ mode might cause more devastation in the coastal region. The further analysis investigated the asymmetry in positive and negative phases of the PJ pattern impact on ocean surface waves. The positive phase is associated with reduced wind-driven wave growth and increased dominance of swells in the BoB, while the negative phase enhances wave growth in the WNP and NIO regions. Composite analysis reveals asymmetry between positive and negative PJ phase impacts, with the negative phase exhibiting a stronger influence on ocean surface waves, suggesting a more pronounced influence of cyclonic circulation and negative SLP anomalies. Understanding the asymmetrical/symmetrical behaviour of the PJ pattern and its impact on ocean surface waves is essential for improving seasonal predictive capabilities and wave forecasting around the Indo-Western Pacific rim countries, complementing existing knowledge on interannual climate modes.

Acknowledgements

We acknowledge the European Centre for Medium-Range Weather Forecasts (ECMWF) for providing reanalysis data (ERA5) which can be accessible at <https://cds.climate.copernicus.eu/cdsapp#!/dataset>. We acknowledge the Director, CSIR- NIO for his support. Figures are prepared using PyFerret software. This is a contribution of NIO xx.

Data availability

The data supporting the findings of this study is freely available on the ERA5 webpage (<https://cds.climate.copernicus.eu/cdsapp#!/dataset>) and the scrips are with the corresponding author available upon valid request.

Declaration of competing interest

The authors declare that they have no known competing financial interests or personal relationships that could have appeared to influence the work reported in this paper.

References

- An, S.I., Park, H.J., Kim, S.K. *et al.* Main drivers of Indian Ocean Dipole asymmetry revealed by a simple IOD model. *npj Clim Atmos Sci* **6**, 93 (2023). <https://doi.org/10.1038/s41612-023-00422-2>
- An, S.-I., and F.-F. Jin, 2004: Nonlinearity and asymmetry of ENSO. *J. Climate*, **17**, 2399–2412, [https://doi.org/10.1175/1520-0442\(2004\)017<2399:NAAOE>2.0.CO;2](https://doi.org/10.1175/1520-0442(2004)017<2399:NAAOE>2.0.CO;2).
- Anoop, T.R., Sanil Kumar, V., Shanas, P.R. and Johnson, G. (2015) Surface wave climatology and its variability in the North Indian Ocean based on ERA-interim reanalysis. *Journal of Atmosphere Ocean Technology*, **32**, 1372–1385. <https://doi.org/10.1175/JTECH-D-14-00212.1>

- Anoop, T.R., Sanil Kumar, V., Shanas, P.R., Glejin, J. and Amrutha, M.M. (2016) Indian Ocean dipole modulated wave climate of eastern Arabian Sea. *Ocean Sciences*, 12, 369–378. <https://doi.org/10.5194/os12-369-2016>.
- Chen W, Zhang R, Wu R, Wen Z, Zhou L, Wang L, Hu P, Ma T, Piao J, Song L, Wang Z, Li J, Gong H, Huangfu J, Liu Y. Recent Advances in Understanding Multi-scale Climate Variability of the Asian Monsoon. *Adv Atmos Sci*. 2023 May 20:1-28. doi: 10.1007/s00376-023-2266-8. Epub ahead of print. PMID: 37359908; PMCID: PMC10199452.
- Chowdary JS, Patekar DD, Srinivas G, Gnanaseelan C, Parekh A (2019) Impact of the Indo-Western Pacific Ocean Capacitor mode on South Asian summer monsoon rainfall. *Clim Dyn* 53(3–4):2327–2338. <https://doi.org/10.1007/s00382-019-04850-w>
- Darshana, P., Chowdary, J.S., Parekh, A. *et al.* Relationship between the Indo-western Pacific Ocean capacitor mode and Indian summer monsoon rainfall in CMIP6 models. *Clim Dyn* **59**, 393–415 (2022). <https://doi.org/10.1007/s00382-021-06133-9>
- Dimri, V.P., Srivastava, R.P. and Pandey, O.P., 2023. Measuring Indian coastline using optimum scale: a case study. *Marine Geophysical Research*, 44(2), p.8.
- Du Y, Xie SP, Huang G, Hu K (2009) Role of air-sea interaction in the long persistence of El Niño-induced north Indian Ocean warming. *J Clim* 22:2023–2038. <https://doi.org/10.1175/2008jcli2590.1>
- Du Y, Chen Z, Xie S-P, Zhang L, Zhang Y and Cai Y (2022) Drivers and characteristics of the Indo-western Pacific Ocean capacitor. *Front. Clim.* 4:1014138. doi: 10.3389/fclim.2022.1014138
- Fu, C., Wang, D., Yang, L., Yao, L., Zhou, F., Priyadarshana, T. and Yao, J. (2018) The relationship between significant wave height and Indian Ocean dipole in the equatorial North Indian Ocean. *Ocean Dynamics*, 68, 689–699. <https://doi.org/10.1007/s10236-018-1154-8>.
- Gill, A., 1980: Some simple solutions for heat-induced tropical circulation. *Quart. J. Roy. Meteor. Soc.*, **106**, 447–462, <https://doi.org/10.1002/qj.49710644905>.
- Hemer MA, Church JA, Hunter JR (2010) Variability and trends in the directional wave climate of the Southern Hemisphere. *Int J Climatol* 30:475–491. <https://doi.org/10.1002/joc.1900>
- Hemer MA, Fan Y, Mori N, Semedo A, Wang XL (2013) Projected changes in wave climate from a multi-model ensemble. *Nat Clim Change* 3:471–476
- Hersbach, H., Bell, B., Berrisford, P., Hirahara, S., Horányi, A., Muñoz-Sabater, J., Nicolas, J., Peubey, C., Radu, R., Schepers, D., Simmons, A., Soci, C., Abdalla, S., Abellan, X., Balsamo, G., Bechtold, P., Biavati, G., Bidlot, J., Bonavita, M., De Chiara, G., Dahlgren, P., Dee, D., Diamantakis, M., Dragani, R., Flemming, J., Forbes, R., Fuentes, M., Geer, A., Haimberger, L., Healy, S., Hogan, R.J., Hólm, E., Janisková, M., Keeley, S., Laloyaux, P., Lopez, P., Lupu, C., Radnoti, G., de Rosnay, P., Rozum, I., Vamborg, F., & Villaume, S. (2020) The ERA5 global reanalysis. *Q J R Meteorological Society*, <https://doi.org/10.1002/qj.3803>.
- Hu, P., Chen, W., Chen, S., Yang, R., Wang, L. and Liu, Y., 2024. Revisiting the linkage between the Pacific–Japan pattern and Indian summer monsoon rainfall: The crucial role of the Maritime Continent. *Geophysical Research Letters*, 51(3), p.e2023GL106982.

- Hu, Peng & Chen, Wen & Wang, Lin & Chen, Shangfeng & Liu, Yuyun & Chen, Lingying. (2022). Revisiting the ENSO–monsoonal rainfall relationship: New insights based on an objective determination of the Asian summer monsoon duration. *Environmental Research Letters*. 17. 10.1088/1748-9326/ac97ad.
- Huang, R., and F. Sun, 1992: Impacts of the tropical western Pacific on the East Asian summer monsoon. *J. Meteor. Soc. Japan*, **70**, 243–256, https://doi.org/10.2151/jmsj1965.70.1B_243.
- Izaguirre, C., Méndez, F.J., Menéndez, M. and Losada, I.J., 2011. Global extreme wave height variability based on satellite data. *Geophysical Research Letters*, 38(10).
- Kankara RS, Ramana Murthy MV, Rajeevan M (2018) National Assessment of shoreline changes along Indian coast: Status report for 26 years (1990–2006). NCCR Publication. <http://www.nccr.gov.in>
- Kaur, S., Kumar, P., Weller, E. *et al.* Multi-model ensemble projections of extreme ocean wave heights over the Indian ocean. *Clim Dyn* **56**, 2163–2180 (2021). <https://doi.org/10.1007/s00382-020-05578-8>
- Kosaka Y, Nakamura H (2010) Mechanisms of meridional teleconnection observed between a summer monsoon system and a subtropical anticyclone. Part I: the Pacific–Japan pattern. *J Clim* 23:5085–5108. <https://doi.org/10.1175/2010JCLI3413.1>
- Kosaka Y, Xie S-P, Lau N-C, Vecchi GA (2013) Origin of seasonal predictability for summer climate over the Northwestern Pacific. *Proc Natl Acad Sci USA* 110(19):7574–7579. <https://doi.org/10.1073/pnas.1215582110>
- Kosaka Y (2021) Coupling of the Indian, western North Pacific, and East Asian summer monsoons. In: Chowdary JS, Parekh A, Gnanaseelan C (eds) *Indian summer monsoon variability: El-Nino teleconnections and beyond*. Elsevier Press, Amsterdam, FL, pp 263–286. <https://doi.org/10.1016/B978-0-12-822402-1.00002-8>
- Kubota H, Kosaka Y, Xie S-P (2016) A 117-year long index of the Pacific–Japan pattern with application to interdecadal variability. *Int J Climatol* 36(4):1575–1589. <https://doi.org/10.1002/joc.4441>
- Kumar P, Min SK, Weller E, Lee H, Wang XL (2016) Influence of climate variability on ocean surface wave heights assessed from ERA-Interim and ERA-20C. *J Clim* 29:4031–4046. <https://doi.org/10.1175/JCLI-D-15-0580.1>
- Kumar, P., Kaur, S., Weller, E. and Min, S.K. (2019) Influence of natural climate variability on the extreme ocean surface wave heights over the Indian Ocean. *Journal of Geophysical Research (Ocean)*, 124, 6176–6199. <https://doi.org/10.1029/2019JC015391>.
- Kumar, V. S., Pathak, K. C., Pednekar, P., Raju, N. S. N., and Gowthaman, R.: Coastal processes along the Indian coastline, *Curr. Sci. India*, 91(4), 530–536, 2006.
- Li, Y., F. Liu, and P.-C. Hsu, 2020: Modulation of the intraseasonal variability of Pacific–Japan pattern by ENSO. *J. Meteor. Res.*, 34, 546–558.

- Madden, R.A., Julian, P.R., 1971. Description of Global-Scale Circulation Cells in the Tropics with a 40–50 Day Period. *J. Atmospheric Sci.* 29, 1109–1123. [https://doi.org/10.1175/1520-0469\(1972\)0292.0.CO;2](https://doi.org/10.1175/1520-0469(1972)0292.0.CO;2)
- Marshall AG, Hemer MA, Hendon HH, McInnes KL (2018) Southern annular mode impacts on global ocean surface waves. *Ocean Model* 129:58–74
- Marshall GJ (2003) Trends in the Southern Annular Mode from observations and reanalyses. *J Clim* 16:4134–4143
- Matsuno, T., 1966: Quasi-geostrophic motions in the equatorial area. *J. Meteor. Soc. Japan*, **44**, 25–43, https://doi.org/10.2151/jmsj1965.44.1_25.
- Muhammed, N. and Sanil Kumar, T.V. (2019) Climatology and trends of the Indian Ocean surface waves based on 39-year-long ERA5 reanalysis data. *International Journal of Climatology*, 40, 979–1006. <https://doi.org/10.1002/joc.6251>.
- Nitta T (1987) Convective activities in the tropical western Pacific and their impact on the Northern Hemisphere summer circulation. *J Meteor Soc Jpn* 65(3):373–390. https://doi.org/10.2151/jmsj1965.65.3_373
- Noh, E., Kim, J., Jun, S.-Y., Cha, D.-H., Park, M.-S., Kim, J.-H., & Kim, H.-G. (2021). The role of the Pacific-Japan pattern in extreme heatwaves over Korea and Japan. *Geophysical Research Letters*, 48, e2021GL093990. <https://doi.org/10.1029/2021GL093990>
- Remya PG, Kumar R, Basu S, Sarkar A (2012) Wave hindcast experiments in the Indian Ocean using MIKE 21 SW model. *J Earth Syst Sci* 121:385–392
- Remya, P.G., Kumar, B.P., Srinivas, G. & Nair, T.M.B. (2020) Impact of tropical and extratropical climate variability on Indian Ocean surface waves. *Climate Dynamics*, 54(11), 4919–4933. Available from: <https://doi.org/10.1007/s00382-020-05262-x>
- Sabique L, Annapurnaiah K, Balakrishnan Nair TM, Srinivas K (2012) Contribution of Southern Indian Ocean swells on the wave heights in the Northern Indian Ocean—a modelling study. *J Ocean Eng* 43:113–120
- Schott, F., and J. P. McCreary, 2001: The monsoon circulation of the Indian Ocean. *Progress in Oceanography*, Vol. 51, Pergamon Press, 1–123.
- Sreejith, M., Remya, P. G., Praveen Kumar, B., Srinivas, G., & Balakrishnan Nair, T. M. (2023). Impact of southern annular mode on the Indian Ocean surface waves. *International Journal of Climatology*, 43(16), 7606–7617. <https://doi.org/10.1002/joc.8282>
- Srinivas G, Chowdary JS, Kosaka Y, Gnanaseelan C, Parekh A, Prasad KV (2018) Influence of the Pacific–Japan pattern on Indian summer monsoon rainfall. *J Clim* 31:3943–3958. <https://doi.org/10.1175/JCLI-D-17-0408.1>
- Srinivas G, Remya PG, Kumar BP, Modi A, Nair TMB. The impact of Indian Ocean dipole on tropical Indian Ocean surface wave heights in ERA5 and CMIP5 models. *Int J Climatol*. 2021;1–14. <https://doi.org/10.1002/joc.6900>

- Srinivas, G., J. Vialard, M. Lengaigne, T. Izumo, and E. Guilyardi, 2022: Relative Contributions of Sea Surface Temperature and Atmospheric Nonlinearities to ENSO Asymmetrical Rainfall Response. *J. Climate*, **35**, 3725–3745, <https://doi.org/10.1175/JCLI-D-21-0257.1>.
- Srinivas, G., Remya, P.G., Malavika, S. & Nair, T.M.B. (2020) The influence of boreal summer intra-seasonal oscillations on Indo-western Pacific Ocean surface waves. *Scientific Reports*, 10(1), 12631. Available from: <https://doi.org/10.1038/s41598-020-69496-9>
- Sun Y, Xu HM, Deng JC (2014) Interdecadal variation in Pacific–Japan teleconnection patterns and possible causes (in Chinese). *Chin J Atmos Sci* 38(6):1055–1065
- Sun, X., R. Greatbatch, W. Park, and M. Latif, 2010: Two major modes of variability of the East Asian summer monsoon. *Quart. J. Roy. Meteor. Soc.*, **136**, 829–841, <https://doi.org/10.1002/qj.635>.
- Takemura K and Mukougawa H (2022) A New Perspective of Pacific–Japan Pattern: Estimated Percentage of the Cases Triggered by Rossby Wave Breaking, *Journal of the Meteorological Society of Japan. Ser. II*, 2022, Volume 100, Issue 1, Pages 115-139
- Vethamony, P., Rashmi, R., Samiksha, S.V. and Aboobacker, V.M. (2013) Recent studies on wind seas and swells in the Indian Ocean: a review. *International Journal of Ocean and Climate System*, 4(1), 63–73.
- Webster PJ, Magana VO, Palmer T, Shukla J, Tomas R, Yanai M, Yasunari T (1998) Monsoons: processes, predictability, and the prospects for prediction. *J Geophys Research: Oceans* 103:14451–14510
- Wu, B., T. Li, and T. Zhou, 2010: Relative contributions of the Indian Ocean and local SST anomalies to the maintenance of the western North Pacific anomalous anticyclone during the El Niño decaying summer. *J. Climate*, 23, 2974-2986.
- Xie S-P, Hu KM, Hafner J, Tokinaga H, Du Y, Huang G, Sampe T (2009) Indian Ocean capacitor effect on Indo-western Pacific climate during the summer following El Niño. *J Clim* 22(3):730–747. <https://doi.org/10.1175/2008JCLI2544.1>
- Xie S-P, Kosaka Y, Du Y, Hu K, Chowdary JS, Huang G (2016) Indowestern Pacific ocean capacitor and coherent climate anomalies in post-ENSO summer: a review. *Adv Atmos Sci* 33(4):411–432. <https://doi.org/10.1007/s00376-015-5192-6>
- Zheng C, Li C, Pan J (2018) Propagation route and speed of swell in the Indian Ocean. *J Geophys Res Oceans* 123(1):8–21
- Zhu, Y., Z. Wen, Y. Guo, R. Chen, X. Li, and Y. Qiao, 2020: The characteristics and possible growth mechanisms of the quasi-biweekly Pacific-Japan teleconnection in boreal summer. *Climate Dyn.*, 55, 3363-3380.

Tables

Acronym	Abbreviation
AS	Arabian Sea
BoB	Bay of Bengal
ENSO	El Niño Southern Oscillation
EOF	Empirical Orthogonal Function
Hs	Total significant wave height
Hss	Swell wave height
Hsw	Significant wave height of wind-sea
IO	Indian Ocean
IOD	Indian Ocean Dipole
IPOC	Indo-Pacific Ocean Capacitor
JJA	June-July-August
NIO	North Indian Ocean
PJ	Pacific-Japan
SAM	Southern Annular Mode
SLP	Sea level pressure
SST	Sea surface temperature
TIO	Tropical Indian Ocean
Tp	Total wave period
Tps	Swell wave period
Tpw	Wind wave period
WNP	Western North Pacific

Table 1. List of abbreviations used in the study.

Figures

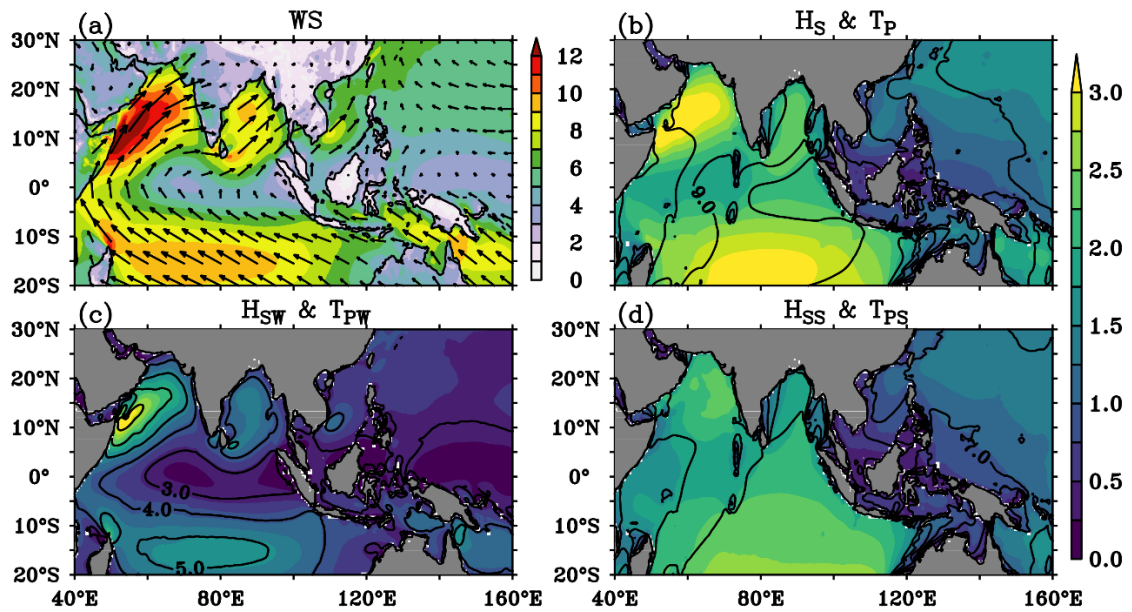


Figure 1. The JJA climatology of (a) surface winds (shaded and vectors; m/s), (b) significant wave height (H_s ; shaded, m) and mean wave period (T_p ; contours, s). Panels (c), and (d) are significant wave heights of wind waves (H_{sw} ; shaded, m) and total swells (H_{ss} ; shaded, m) along with their mean wave periods (contours, s) respectively.

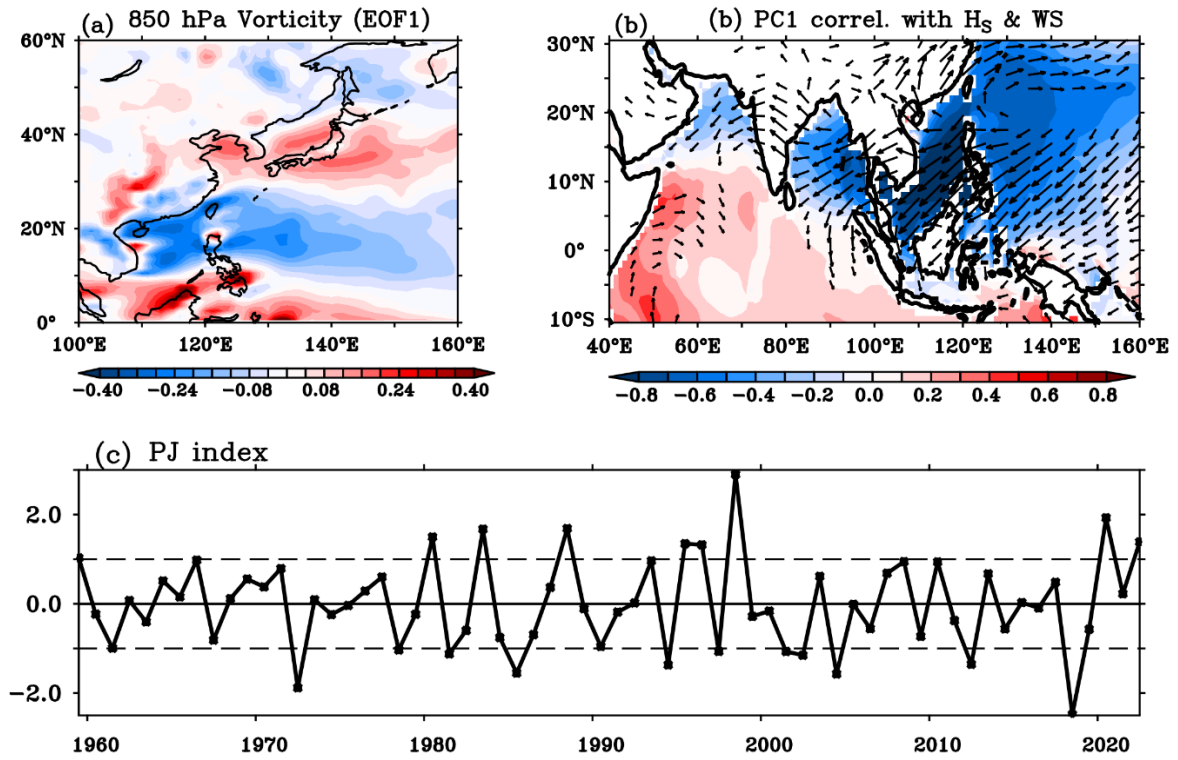


Figure 2. (a) Spatial pattern of Empirical Orthogonal Function first mode (EOF1) of relative vorticity at 850 hPa (10^{-5} s^{-1}), (b) corresponding first principal component (PJ index) correlation with H_s (shaded) and surface wind (vectors) anomalies, and (c) normalized time series of PJ index. The dashed lines show the ± 1 standard deviation of the PJ index.

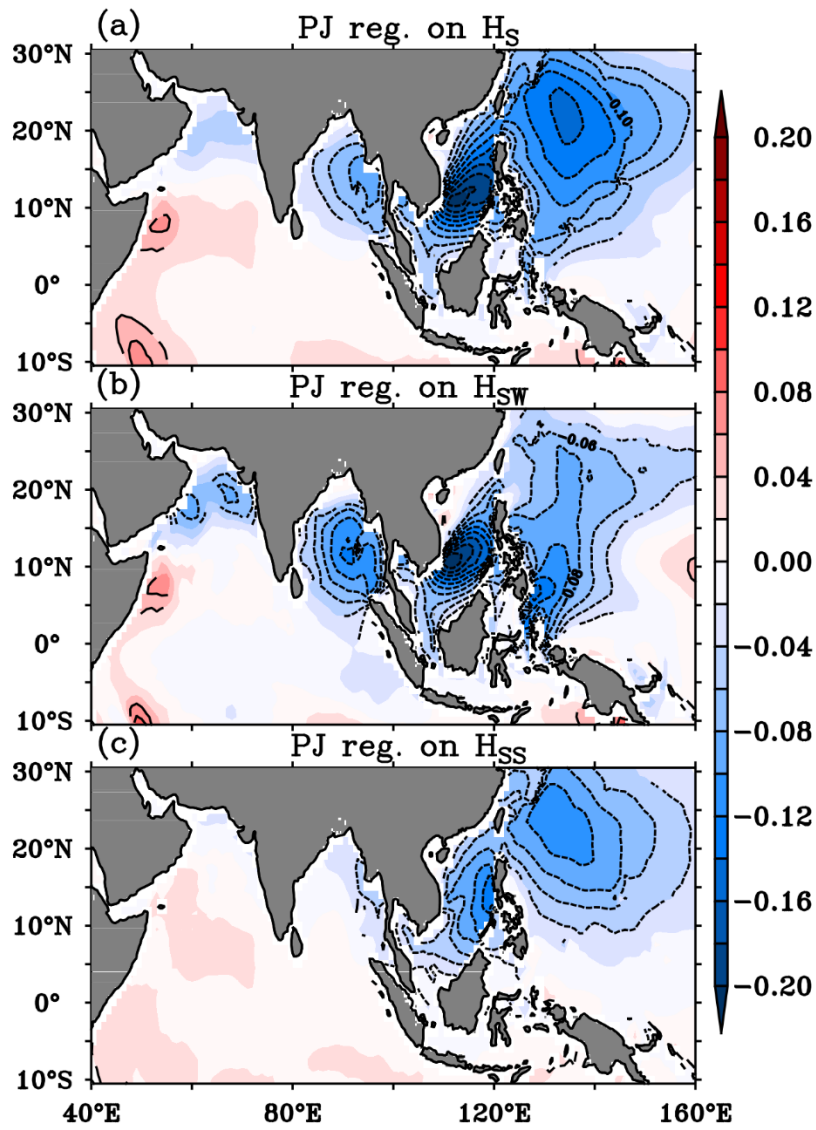


Figure 3. Regression of (a) H_s (m), (b) H_{sw} (m) and (c) H_{ss} (m) anomalies on PJ index. Contours show significance at a 95% confidence level.

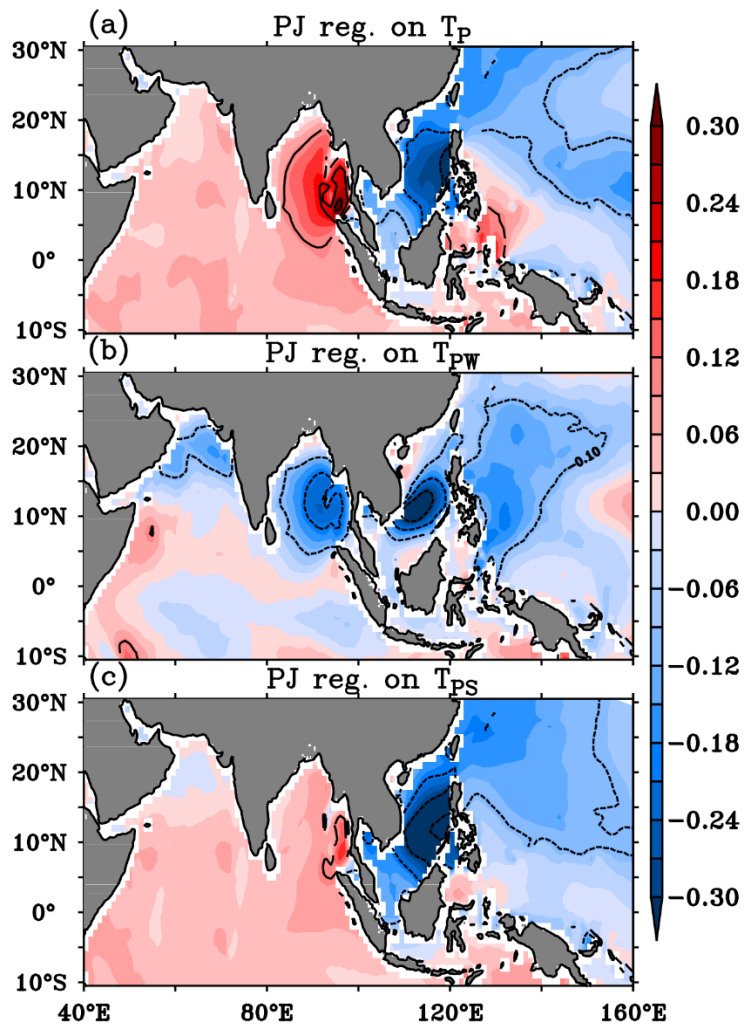


Figure 4. Regression of (a) T_p (s), (b) T_{pw} (s) and (c) T_{ps} (s) anomalies on PJ index. Contours show significance at a 95% confidence level.

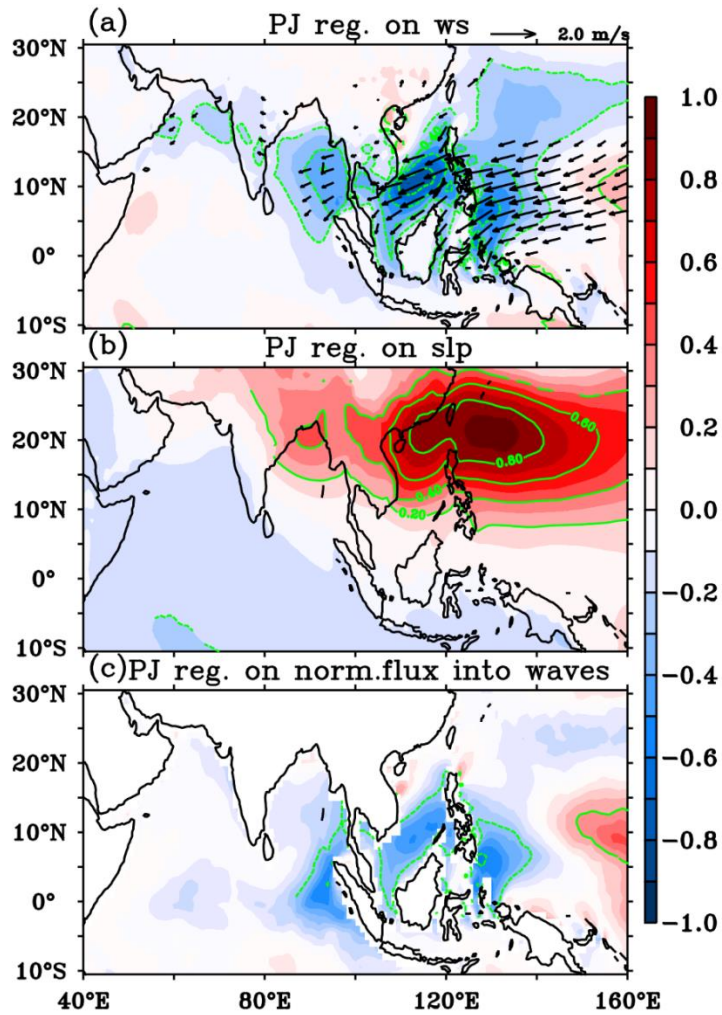


Figure 5. Regression of (a) surface wind speeds (shaded and vectors, m/s), (b) mean sea level pressure (hPa), and (c) normalized energy flux transfer to wave (dimensionless) anomalies. The green contours and vectors show significance at a 95% confidence level.

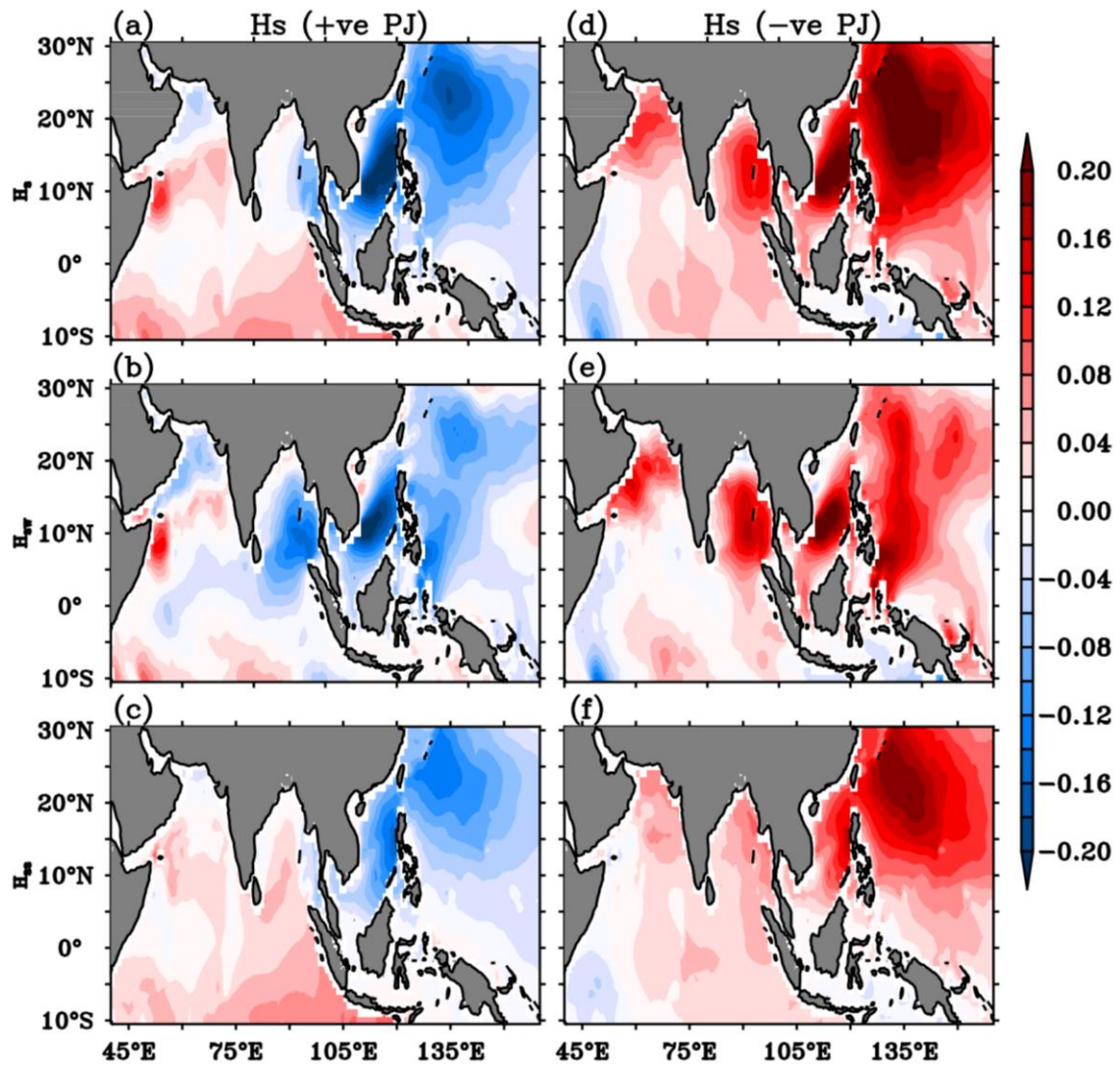


Figure 6. JJA composites of (a) Hs (m), (b) Hsw (m) and (c) Hss (m) anomalies during the positive phase of PJ mode. (d) - (f) same as (a) – (c) but for its negative phase.

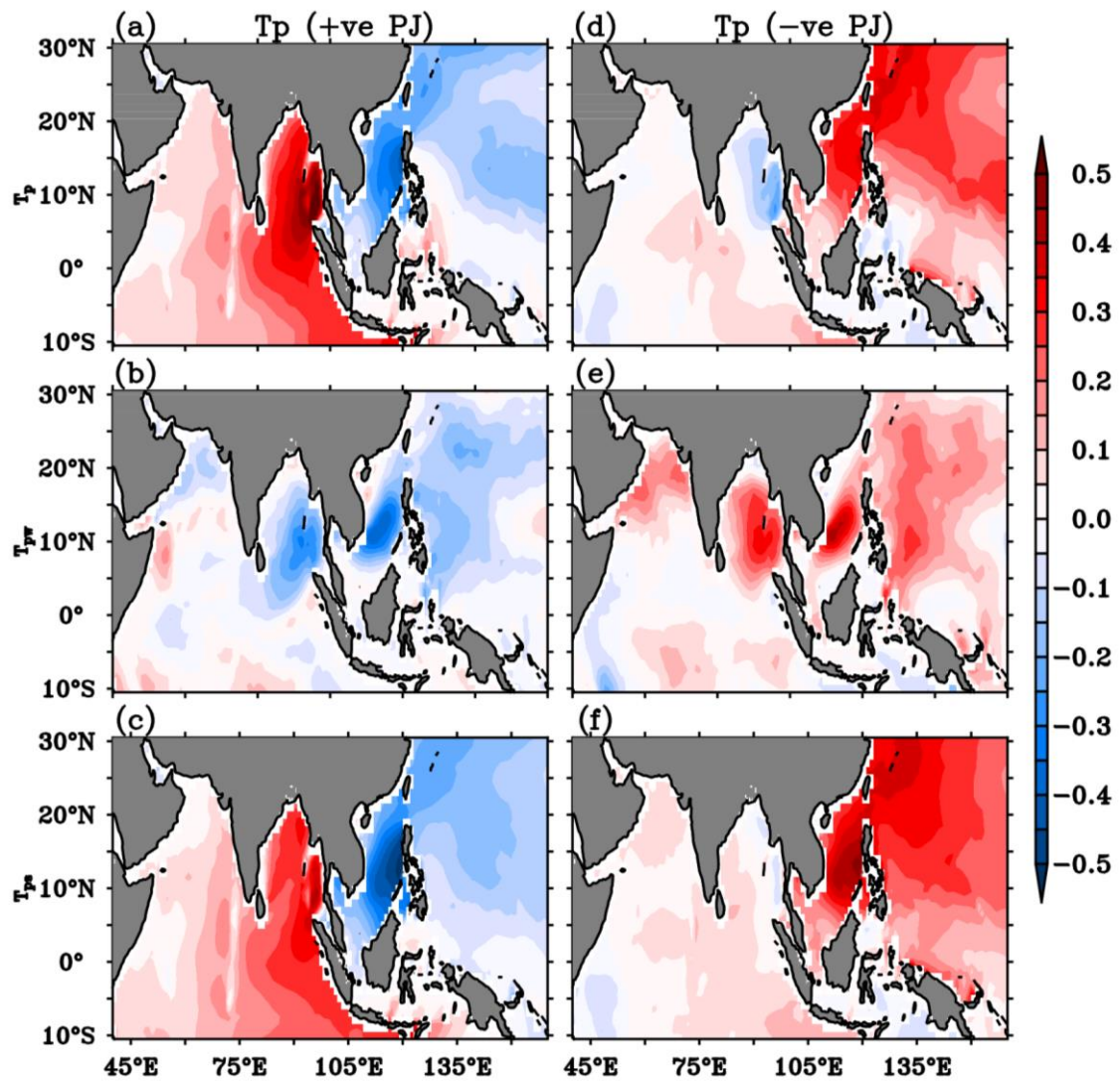


Figure 7. JJA composites of (a) T_p (s), (b) T_{pw} (s) and (c) T_{ps} (s) anomalies during the positive phase of PJ mode. (d) - (f) same as (a) – (c) but for its negative phase.

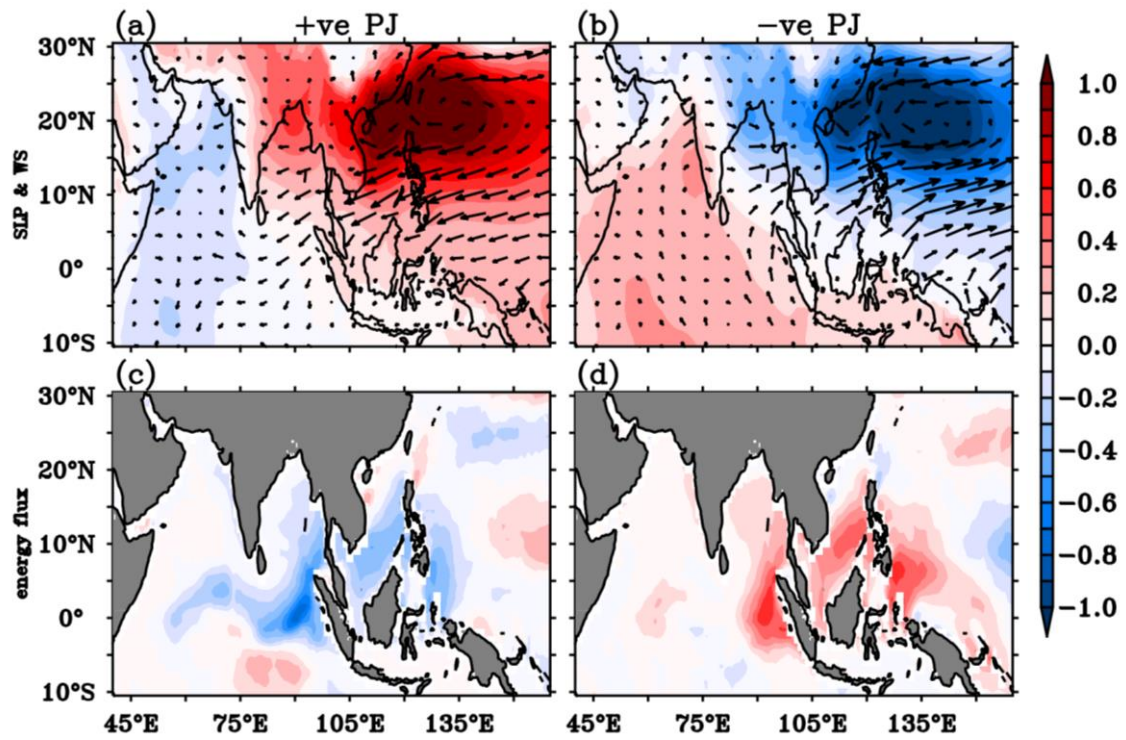


Figure 8. JJA composites of (a) mean sea level pressure (shaded, hPa) and surface winds (vectors, m/s) during positive PJ and (b) negative PJ years. (c) – (d) same as (a) – (b) but for normalized energy flux into wave anomalies (dimensionless).

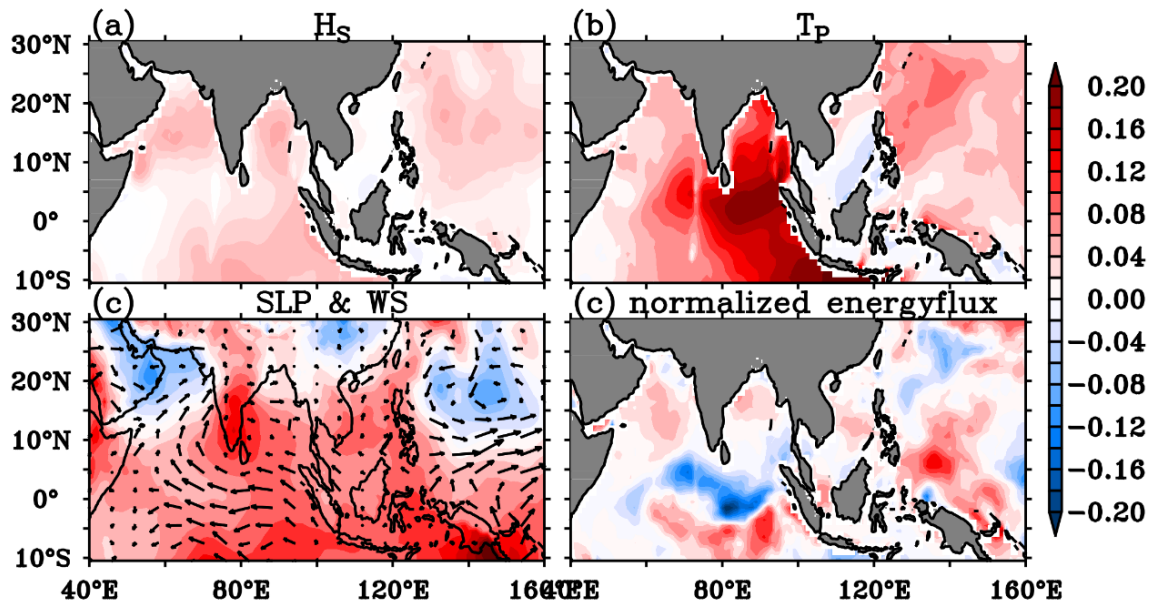


Figure 9. JJA average of PJ asymmetries (half sum of the positive PJ and negative PJ years composites) in **(a)** Hs (shaded, m), **(b)** Tp (shaded, s), **(c)** mean sea level pressure (shaded, hPa) and surface wind (vectors, m/s) and **(d)** normalized energy flux (dimensionless) anomalies.

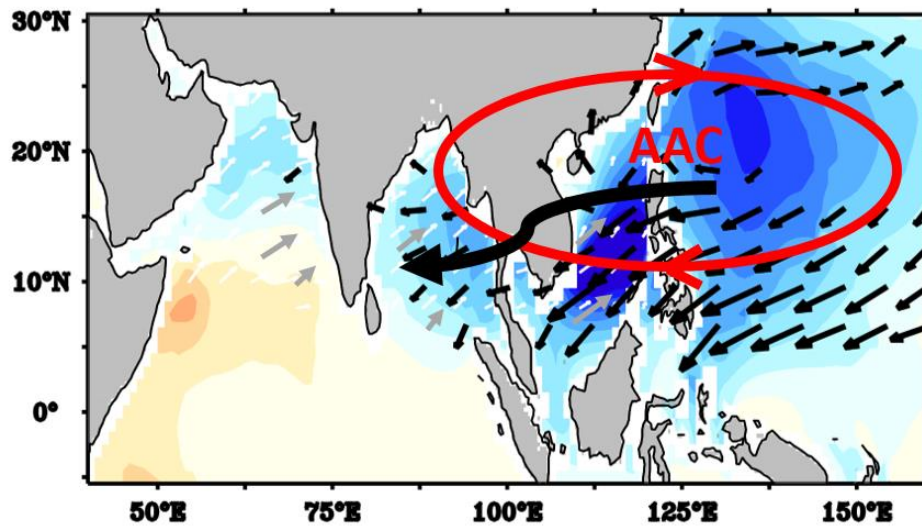


Figure 10. Schematic diagram that shows the PJ impact on Indo-western Pacific significant wave heights. The colour shading represents the Hs anomalies and vectors (black) are surface wind anomalies over the Indo-western Pacific region. The mean south-westerly winds are marked as white/grey vectors. The elliptical red circle shows the anomalous anticyclonic circulation over the BoB and WNP regions. *The southern flank of the anomalous anticyclonic circulation induces the northeasterlies which oppose the mean south-westerlies resulting in the weakening of the wave heights over the WNP and BoB regions in response to the PJ pattern.*